Experimental validation of all-dielectric mm-wave polarization conversion based on form birefringence

Experimental validation of all-dielectric mm-wave polarization conversion based on form birefringence

Maria Lorente-Crespo, *Student Member, IEEE,* Guillem C. Ballesteros, George Goussetis, *Senior Member, IEEE* and Carolina Mateo-Segura, *Member, IEEE*

***Abstract*—In this contribution, a mm-wave all-dielectric linear-to-circular polarization converter is reported for the first time. The proposed converter consists of a periodic stack of isotropic dielectric substrates that produces form birefringence. By virtue of the anisotropy of the permittivity tensor, the phase-shift introduced between two orthogonally linearly polarized transmitted electromagnetic waves can be controlled, enabling linear-to-circular polarization conversion. Due to its all-dielectric nature, the proposed polarization converter circumvents oxidation, corrosion and power handling problems associated with metallic structures. Our measurements demonstrate 17% 1dB axial ratio fractional bandwidth and 39% below 3dB, while measured insertion loss is 0.6dB at the operating frequency. The proposed polarization converter further benefits from angularly stable response up to 40°.**

***Index Terms*—Polarization conversion, birefringence, polarimetry, dielectric frequency selective surfaces**

I. Introduction

POLARIZATION converters play a key role in a broad variety of applications within the radio frequency and microwave frequency bands of the electromagnetic spectrum. Their role in millimeter (mm) and sub-mm imaging systems for concealed weapon detection [1], environmental monitoring [2] and as isolators for protecting amplifiers [3], is particularly relevant. Likewise, polarization converters may also be encountered in satellite communication links in order to address depolarization and misalignment effects [4].

In general, circular polarization (CP) can be obtained by placing a polarization converter operating in the transmit mode in front of a linearly polarized (LP) antenna or integrating the converter with a metallic ground plane when operating in reflection. In both configurations, LP-to-CP conversion usually involves arrays of metallic elements. This is the case of frequency selective surfaces [2], anisotropic high impedance surfaces [5] and lamellar gratings [6], among others. However, structures consisting of such metallic grids suffer from power handling issues, oxidation and corrosion problems [7]. Furthermore, as the operating frequency band increases, the etching of the metallic layers becomes more expensive and critical, complicating substantially the fabrication process.

All-dielectric polarization converters, as those used in optics, may overcome these limitations. Predominantly, the conversion is achieved using birefringent crystals with appropriate dimensions and orientation (quarter-plates) exhibiting frequency dispersive anisotropy of the permittivity tensor [8]. In microwaves, the level of birefringence available in natural media limits their practical application. However, increased birefringence can be realized artificially by virtue of arranging different dielectrics (form birefringence) [8]. In this letter, based on the concept proposed in [9], we report the first experimental mm-wave all-dielectric LP-to-CP polarization converter.

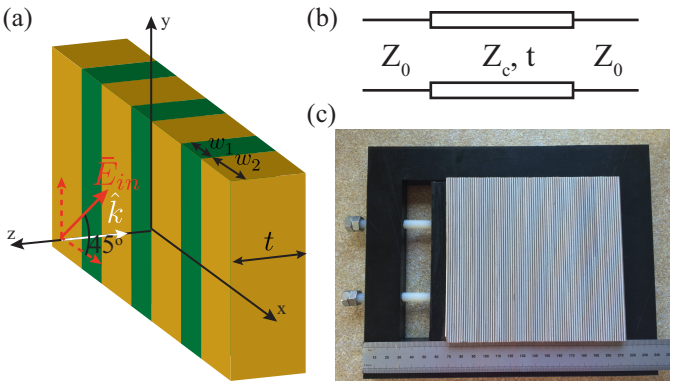

Fig. 1. (a) Proposed structure. The dielectric stack extends to infinity in the y-direction and is repeated periodically along $\hat{x}$. An incoming plane-wave propagating along $-\hat{z}$ whose E-field is contained in the xy-plane impinges the structure. (b) Equivalent circuit model.(c) Fabricated prototype consisting of 80 pairs of dielectrics (foam/PTFE) enclosed by an adjustable plastic frame with nylon screws.

II. Principle of Operation and Design

The proposed mm-wave LP-to-CP polarization converter is based on form birefringence. The structure consists of a sub-wavelength periodic stack of dielectric sheets with permittivities ϵ_1 and ϵ_2, and widths w_1 and w_2, respectively, Fig. 1(a). In the metamaterial regime, i.e. when the period w_1+w_2 is smaller than the free-space wavelength of operation, the electromagnetic characteristics of the structure can be described using an effective medium approximation [8]. In this case, electromagnetic waves interact with the structure as they would with a bulk medium with an effective in-plane anisotropic permittivity. If a normal incident LP plane-wave with E-field $\vec{E} = E_x\hat{x} + E_y\hat{y}$ impinges the structure

M. Lorente-Crespo, G. Goussetis and C. Mateo-Segura are with the Institute of Sensors, Signals and Systems, Heriot-Watt University, Edinburgh, EH14 4AS, U.K. (e-mail: ml343@hw.ac.uk, g.goussetis@hw.ac.uk, c.mateo-segura@hw.ac.uk)

G. C. Ballesteros is with the Institute of Photonics and Quantum Sciences, SUPA, Heriot-Watt University, Edinburgh, EH14 4AS, U.K. (e-mail: gb173@hw.ac.uk)

This work was supported by FP7 project DORADA (IAPP-2013-610691) and by EPSRC (EP/L015110/1). Thanks to Taconic Advanced Dielectric Division for providing the dielectric material.

in Fig. 1(a), each component of the E-field will encounter a different effective permittivity, ϵ_{xx} and ϵ_{yy} , given by [8]

$$\epsilon_{xx} = \left(\frac{v_1}{\epsilon_1} + \frac{v_2}{\epsilon_2}\right)^{-1}, \tag{1}$$

$$\epsilon_{yy} = v_1\epsilon_1 + v_2\epsilon_2, \tag{2}$$

where v_1 and v_2 are the volume fractions occupied by each dielectric medium and $\epsilon_{yy} > \epsilon_{xx}$.

From an equivalent network perspective the converter can be modelled as a transmission line with length t, characteristic impedance Z_c and symmetric port impedance Z_0, Fig. 1(b). The reflection coefficient of the air-dielectric interface is

$$r = \frac{Z_c - Z_0}{Z_c + Z_0}, \tag{3}$$

where the characteristic impedance of the equivalent transmission line is that of the effective dielectric $Z_c = Z_0/\sqrt{\epsilon_r}$ and Z_0 corresponds to the free-space impedance. The ABCD-matrix of the equivalent transmission line is [10]

$$\begin{bmatrix} A & B \\ C & D \end{bmatrix} = \begin{bmatrix} \cosh(\phi) & Z_c \sinh(\phi) \\ \sinh(\phi)/Z_c & \cosh(\phi) \end{bmatrix} \tag{4}$$

where the accumulated phase-shift upon transmission through the circuit is $\phi = t\sqrt{\epsilon_r}\omega/c$. Given the ABCD representation, the S-parameters can be easily computed algebraically. In particular, the transmission S-parameter in (5) can be obtained using the relation $S_{21} = 2/(A + B/Z_0 + CZ_0 + D)$ [10]

$$S_{21} = \frac{\left(1 - r^2\right)\exp[-j\phi]}{1 - r^2\exp[-2j\phi]} \tag{5}$$

In the above, the relative permittivity ϵ_r depends on the polarization of the propagating E-field. For the x-polarization this is described by (1) while for the y-polarization it is given by (2). As a result, the two E-field components propagate through the structure with different phase velocities. Finally, the phase-delay between both field components can be obtained from (5).

To gain better physical intuition, reflections at the input and output interfaces may be neglected by equating (3) to zero. In this scenario, the phase delay can be simplified to

$$\Delta = \frac{\omega}{c} t \left(\sqrt{\epsilon_{yy}} - \sqrt{\epsilon_{xx}}\right). \tag{6}$$

When $\Delta = 90^o$, a CP wave with E-field $\vec{E} = E_x\hat{x} + jE_y\hat{y}$ and $|E_x| = |E_y|$ will be obtained at the output. This indicates that in order to realize a compact LP-to-CP converter, a high contrast between ϵ_1 and ϵ_2 is required. This gives rise to a compromise between thickness and insertion loss (IL). For those applications in which IL is not a constraint, the thickness could be considerably reduced to achieve very compact devices.

III. Experiment and Results

A prototype (Device Under Test: DUT) was fabricated using alternating layers of $w_1 = 0.95$-mm-wide ROHACELL 31 HF rigid foam and $w_2 = 0.8$-mm-wide Taconic TLY-5 PTFE, as shown in Fig. 1(c). The lateral dimensions were 135 mm $\times$144 mm or equivalently $15\lambda \times 16\lambda$, where λ corresponds to 33.25 GHz, so that edge effects were minimized. The adjustable plastic frame with nylon screws provides the necessary mechanical stability while minimizing reflections. The electric permittivity of both materials was characterised at the central frequency [11]. These were found to be $\epsilon_1 = 1.21$ and $\epsilon_2 = 2.77$. These two media cause the effective dielectric constants in (1) and (2) to be $\epsilon_{xx} = 1.63$ and $\epsilon_{yy} = 1.92$, thus minimizing loses through better free-space matching, and the estimated loss tangent $\tan(\delta_{xx}) = 0.0046$ and $\tan(\delta_{yy}) = 0.0072$. The thickness of the converter was $t = 19.4$ mm. According to (6), this will allow a 90° phase shift at 34.8 GHz.

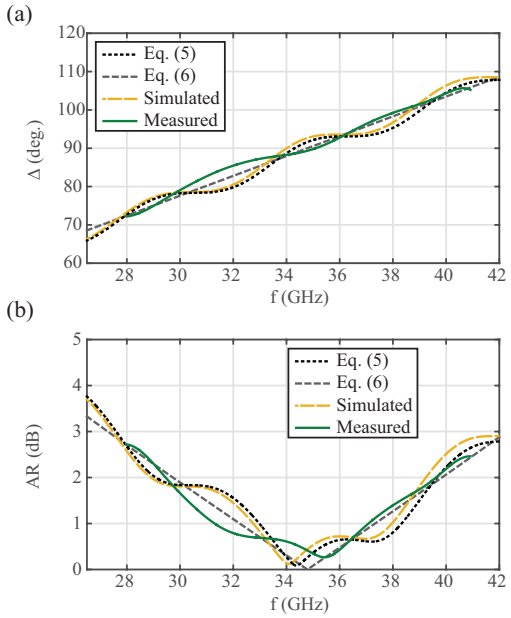

Fig. 2. (a) Phase-shift and (b) realized AR when a normal incident LP plane-wave travels through DUT obtained using the analytical model (5), its simplified version (6), CST simulations and measurements of the fabricated prototype.

The measurement set-up consisted of two Ka-band linearly polarized standard-gain Flann horn antennas positioned 80 cm away from each other acting as the transmitter and the receiver. The DUT was located at the central position. A PNA Microwave Network Analyzer (Agilent N5225A) was used to measure the magnitude and phase of the transmission coefficient. In order to filter background noise (e.g. reflections in the connectors and losses in the cables), time-gating using a 0.6 μs Hann window was applied to the measured S-parameters. No multipath interference was identified. From the measurements, the axial ratio (AR), which evaluates the purity of circular polarization, can be readily obtained [5].

Fig. 2(a) and Fig. 2(b) show a comparison of the phase-shift and AR values obtained using the analytical model described by (5), its simplified version (6), CST Microwave Studio and measurements. In all the cases a normal incident LP plane-wave is considered to travel through the DUT and a very good agreement is observed. In the simulations, the dielectrics were assumed lossless. Since in the designed converter reflections at the interfaces are nearly negligible (measured $S_{11} < -19$dB), i.e. the converter is nearly perfectly matched to free-space, results obtained using (5) and (6) agree remarkably well. The

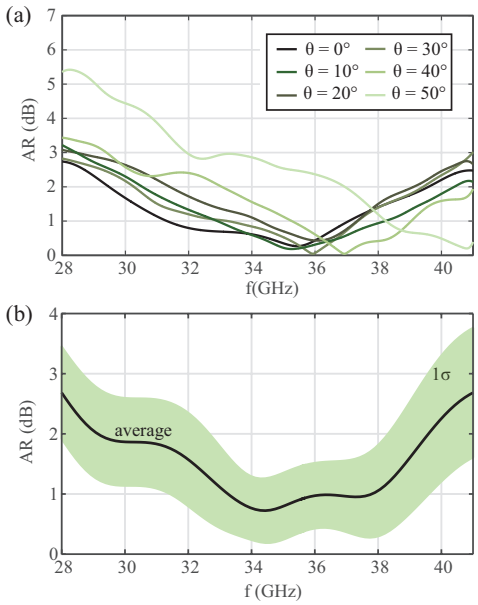

Fig. 3. (a) Measured AR for $\theta = 0 - 50°$ incidence. (b) Sensitivity analysis to random variations of ϵ_1 and ϵ_2.

effect of the impedance mismatch arises as an increased ripple with respect to the simplified analytical results. However, the proposed model predicts accurately the spectral response of the converter albeit its simplicity. Results obtained using (5) are nearly identical to those obtained through CST simulations. Small differences are appreciated as the frequency increases due to the limited validity of the effective medium approximation. Likewise, the agreement with the measurements is good. The minimum measured AR is 0.27dB at 35.5 GHz (2% operating frequency shift attributed to fabrication tolerances). The measured 3dB AR fractional bandwidth is 39% while the 1dB AR bandwidth is approximately 17%. Similarly to traditional quarter-plates, the retardation introduced between E_x and E_y is equal to 90° at a single frequency, 35.2 GHz, which is very close to the operating frequency, Fig. 2. This indicates that the magnitude of E_x and E_y are nearly identical, which is also a requirement for getting pure CP. IL calculated from the measured transmission parameter normalized to the case of free-space propagation is $\sim$ 0.6dB at the operating frequency which is similar to current state-of-the art technologies [1]. The latter property together with the low reflections achieved, make the proposed converter particularly suitable for its integration in antenna systems.

The sensitivity of the structure is investigated in Fig. 3. Specifically, Fig. 3(a) shows the measured AR when the angle of incidence varies between $\theta = 0 - 50°$. As can be seen, the response is remarkably stable up to 30°. As the angle of incidence increases further, the minimum AR shifts towards higher frequencies. For instance, $\theta = 40°$ causes a 4% frequency deviation, whilst $\theta = 50°$ yields 15%. In terms of bandwidth, the response of the DUT remains mostly unaltered whilst the IL is kept below 1.5dB for $\theta < 50°$. Additionally, the AR sensitivity due to variations of ϵ_1 and ϵ_2 is studied in Fig. 3(b). There, the 1-σ confidence interval and the average

TABLE I
COMPARISON WITH EXISTING TECHNOLOGIES

Ref.	Ours	[1]	[2]	[3]	[5]
f (GHz)	35.5	95	325	8.83	12.6
Bandwidth (%)	39	5	12	-	63
AR (dB)	0.27	0.23	0.19	2.5	0.7
Angular Stability (°)	0-40	0-17	-	-	0-45
IL (dB)	0.6	0.3	3.4	2	-

AR calculated using a Montecarlo analysis considering a 2% standard deviation from ϵ_1 and ϵ_2 have been depicted. Our results show that the performance of the converter is robust against small fluctuations in the dielectric constant which may be caused in practice by temperature variations or mechanical stress.

IV. CONCLUSIONS

In conclusion, in this work the first experimental realization of a mm-wave LP-to-CP polarization converter is reported. The required birefringence is achieved by periodically stacking two different dielectric substrates. Fabrication techniques such as 3D-printing technology may also be employed. A comparison with previous converters is given in Table I. The prototype presented here outperforms existing converters in terms of AR [3], [5] and bandwidth [1], [2]. Our measurements indicate that the converter exhibits good angular stability, comparable to [5] and IL similar to that of state-of-the-art technologies [1].

REFERENCES

[1] C. Dietlein, A. Luukanen, Z. Popovic, and E. Grossman, "A W-band polarization converter and isolator," *IEEE Trans. Antennas and Propag.*, vol. 55, no. 6, pp. 1804–1809, June 2007.
[2] M. Euler, V. Fusco, R. Cahill, and R. Dickie, "325 GHz single layer sub-millimeter wave FSS based split slot ring linear to circular polarization convertor," *IEEE Trans. Antennas Propag*, vol. 58, no. 7, pp. 2457–2459, July 2010.
[3] S. Hollung, W. Shiroma, M. Markovic, and Z. Popovic, "A quasi-optical isolator," *IEEE Microw. Guided Wave Lett*, vol. 6, no. 5, pp. 205–206, May 1996.
[4] N. Fonseca and C. Mangenot, "High-performance electrically-thin dual-band polarizing reflective surface for broadband satellite applications," *IEEE Trans. Antennas Propag.*, vol. PP, no. 99, pp. 1–1, 2015.
[5] E. Doumanis, G. Goussetis, J. Gomez-Tornero, R. Cahill, and V. Fusco, "Anisotropic impedance surfaces for linear to circular polarization conversion," *IEEE Trans. Antennas Propag*, vol. 60, no. 1, pp. 212–219, Jan 2012.
[6] C. W. Haggans, L. Li, T. Fujita, and R. K. Kostuk, "Lamellar gratings as polarization components for specularly reflected beams," *J. of Mod. Opt.*, vol. 40, no. 4, pp. 675–686, Mar 1993.
[7] A. Jain, P. Tassin, T. Koschny, and C. M. Soukoulis, "Large quality factor in sheet metamaterials made from dark dielectric meta-atoms," *Phys. Rev. Lett.*, vol. 112, p. 117403, Mar 2014.
[8] M. Born and E. Wolf, *Principles of Optics: Electromagnetic theory of propagation interference and diffraction of light*, 6th ed. Cambridge University Press, 1993.
[9] M. Lorente-Crespo, G. Ballesteros, and C. Mateo-Segura, "All-dielectric broadband microwave polarization conversion based on form birefringence," in *Advanced Electromagnetic Materials in Microwaves and Optics (METAMATERIALS), 2015 9th International Congress on*, Sept 2015, pp. 184–186.
[10] D. M. Pozar, *Microwave Engineering*. John Wiley & Sons, 2005.
[11] I. Zivkovic and A. Murk, "Free-space transmission method for the characterization of dielectric and magnetic materials at microwave frequencies," in *Microwave Materials Characterization*, P. S. Costanzo, Ed. InTech, 2012, ch. 5.